Video Article

Dual-mode Imaging of Cutaneous Tissue Oxygenation and Vascular Function

Ronald X. Xu[1], Kun Huang[2], Ruogu Qin[1], Jiwei Huang[1], Jeff S. Xu[1], Liya Ding[2], Urmila S. Gnyawali[3], Gayle M. Gordillo[3], Surya C. Gnyawali[3,4], Chandan K. Sen[3]

[1]Department of Biomedical Engineering, The Ohio State University

[2]Department of Biomedical Informatics, The Ohio State University

[3]Comprehensive Wound Center, The Ohio State University

[4]Department of Surgery, The Ohio State University

Correspondence to: Chandan K. Sen at chandan.sen@osumc.edu

URL: http://www.jove.com/video/2095
DOI: doi:10.3791/2095

Keywords: Medicine, Issue 46, Dual-mode, multispectral imaging, infrared imaging, cutaneous tissue oxygenation, vascular function, co-registration, wound healing

Date Published: 12/8/2010

Citation: Xu, R.X., Huang, K., Qin, R., Huang, J., Xu, J.S., Ding, L., Gnyawali, U.S., Gordillo, G.M., Gnyawali, S.C., Sen, C.K. Dual-mode Imaging of Cutaneous Tissue Oxygenation and Vascular Function. *J. Vis. Exp.* (46), e2095, doi:10.3791/2095 (2010).

Abstract

Accurate assessment of cutaneous tissue oxygenation and vascular function is important for appropriate detection, staging, and treatment of many health disorders such as chronic wounds. We report the development of a dual-mode imaging system for non-invasive and non-contact imaging of cutaneous tissue oxygenation and vascular function. The imaging system integrated an infrared camera, a CCD camera, a liquid crystal tunable filter and a high intensity fiber light source. A Labview interface was programmed for equipment control, synchronization, image acquisition, processing, and visualization. Multispectral images captured by the CCD camera were used to reconstruct the tissue oxygenation map. Dynamic thermographic images captured by the infrared camera were used to reconstruct the vascular function map. Cutaneous tissue oxygenation and vascular function images were co-registered through fiduciary markers. The performance characteristics of the dual-mode image system were tested in humans.

Video Link

The video component of this article can be found at http://www.jove.com/video/2095/

Protocol

1. Mapping tissue oxygenation by multispectral imaging

A Comprehensive Wound Center (CWC) dual-mode imaging system, henceforth referred to as the CWC system, was developed at the Ohio State University for multispectral imaging of cutaneous tissue oxygenation and thermographic imaging of vascular function. The wide gap second derivative spectroscopic technique was used to reconstruct tissue oxygenation maps based on multispectral images [1]. In this study, a healthy subject sat with the left forearm resting on a countertop. A portion of the forearm within the field of view of the CWC system was painted with India ink (1% dissolved in ethanol) to mimic different skin colors. Multispectral images were acquired and an oxygenation map was reconstructed based on the wide gap second derivative spectrum. The reconstructed oxygenation map was compared with that acquired by a commercial Hypermed OxyVu hyperspectral tissue oxygenation measurement system.

Tissue oxygen responses to vascular occlusion were studied on the same subject following a protocol of post-occlusive reactive hyperemia (PORH) [2]. Before the PORH test, the subject's systolic and diastolic blood pressures were recorded by a pressure cuff placed on the left upper arm. The PORH protocol consisted of a pre-occlusive baseline period of two minutes, a suprasystolic occlusion (systolic + 50 mm Hg) period of two minutes, and a reactive hyperemia period of two minutes. Multispectral images were acquired at four wavelengths (i.e., 530nm, 550nm, 570nm, and 590nm) during the PORH test at the sampling rate of 0.75 seconds per wavelength. Deep tissue oxygen saturation and cutaneous tissue oxygen tension on the same arm were simultaneously recorded by an OxiplexTS tissue spectrophotometer (ISS Inc., Urbana Champaign, IL) and a TCM transcutaneous oxygen monitor (Radiometer, Denmark) respectively.

2. Mapping vascular function by dynamic thermographic imaging

Dynamic thermographic imaging was demonstrated on a healthy subject using the same CWC system. The subject comfortably lied on a table in supine position, with the left arm resting on a countertop and the dorsum of the left hand facing up toward the infrared camera unit of the CWC system. A laser Doppler probe was placed on the finger tip of the same hand for continuous monitoring of finger skin perfusion. A pressure cuff was placed on the left upper arm to produce different levels of occlusion. Before the experiment, the subject was asked to rest for at least 10 minutes, with the systolic and diastolic pressures recorded by the pressure cuff. Dynamic thermographic images were captured at the following cuff pressure levels: no occlusion, 0.5 x diastolic blood pressure, 0.5 x (diastolic blood pressure + systolic blood pressure), and 1.5 x systolic blood pressure. At each cuff pressure level, a thermal stimulation was introduced by placing a water bag of room temperature (25°C) on the left hand for 30 seconds. Immediately after the removal of the thermal stimulation, the left hand thermographic images were acquired at a rate of 2 frames/second and the finger skin perfusion was recorded by the laser Doppler probe at the sampling rate of 10 Hz. The time interval between tests was 10 min. The position of the left hand was marked in advance so that the subsequent measurements were at the same position. Tissue vascular functions at different occlusion levels were evaluated by calculating both the temperature response and the vascular function index. The vascular function index was defined as the ratio between the square root of the time after thermal stimulation and the corresponding temperature change.

3. Co-registration between tissue oxygenation and vascular function maps

The map of cutaneous tissue vascular function acquired by dynamic thermographic imaging and the map of cutaneous tissue oxygenation acquired by multispectral imaging were co-registered by an advanced imaging algorithm. Four fiduciary markers, with simultaneous thermal and optical contrasts, were placed on the biological tissue to facilitate image co-registration. Currently the protocol for co-registering the optical image (and the oxygenation map) with the thermal image (and the vascular function map) includes the following key steps: 1) transform all the images to gray scale and normalize the pixel intensity values between 0 and 1; 2) for the optical photo, identify the foreground (skin) region which has high pixel intensity values than the an empirical global threshold (0.8 times the mean intensity value of the whole image); the small holes in the foreground region were filled using the morphological close operation; 3) identify the fiduciary marker regions as darker regions in the foreground whose intensity values are below both the global threshold and the adaptive local threshold defined by the mean pixel values in the 20-by-20 pixel neighborhood. The adaptive local threshold allowed us to accommodate the illumination variation; 4) refine the fiduciary marker regions using morphological operations to remove noise and spikes; the centroids of the four regions were selected as control points in the optical photo; 5) repeat similar steps to identify marker regions in the thermal image; 6) match the two sets of control points based on proximity (given that the two cameras were closely positioned); 7) compute an affine transformation between the two images with the thermal image as the reference and transform the optical photo and the oxygen map (which is obtained from the same camera as the optical photo) correspondingly; 8) finally generate the overlaid images for visualization.

4. Representative Results:

The representative results for the oxygenation protocol (i.e., #1) are cutaneous tissue oxygenation maps reconstructed based on wide gap second derivative spectroscopy. The method of wide gap second derivative spectroscopy effectively reduced the measurement artifacts caused by tissue background absorption so that the cutaneous oxygenation measurement was less affected by the simulated skin color changes. We also demonstrated a PORH protocol where the cutaneous tissue oxygenation map, the deep tissue oxygenation, and the cutaneous tissue oxygen tension were simultaneously recorded.

The representative results for the vascular function protocol (i.e., #2) include the cutaneous tissue temperature distributions, the cutaneous tissue temperature changes in response to external thermal stimulation, and the cutaneous tissue vascular index maps derived from dynamic thermographic imaging. Correlations were observed between the thermographic imaging of cutaneous tissue vascular index and the laser Doppler measurement of skin tissue perfusion.

The representative results for the co-registration protocol (i.e., #3) include the tissue oxygenation map, the vascular index map, and the image fusion among photographic, oxygenation, and vascular index images co-registered by multi-contrast fiduciary markers.

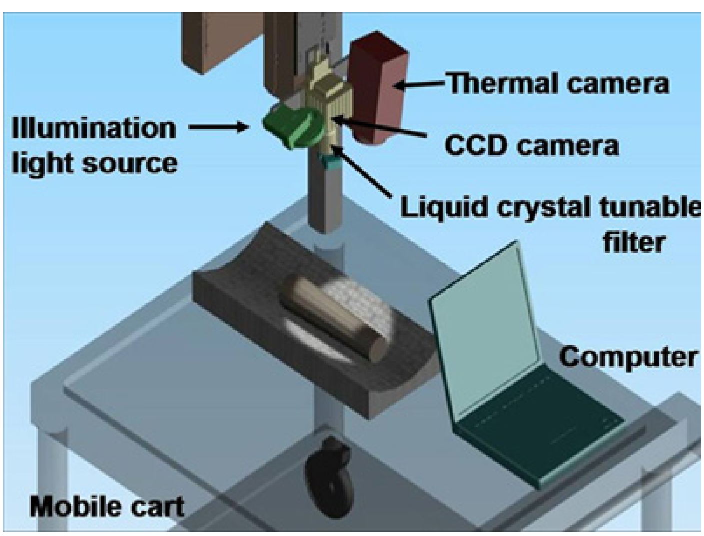

Figure 1. CWC dual-mode system setup for non-contact imaging of tissue oxygenation and vascular function. The system was installed on a mobile cart. It consisted of an infrared thermal camera, a CCD camera, a liquid crystal tunable filter, and a broadband light source. A computer was used to synchronize the tasks of data collection, analysis, and display.

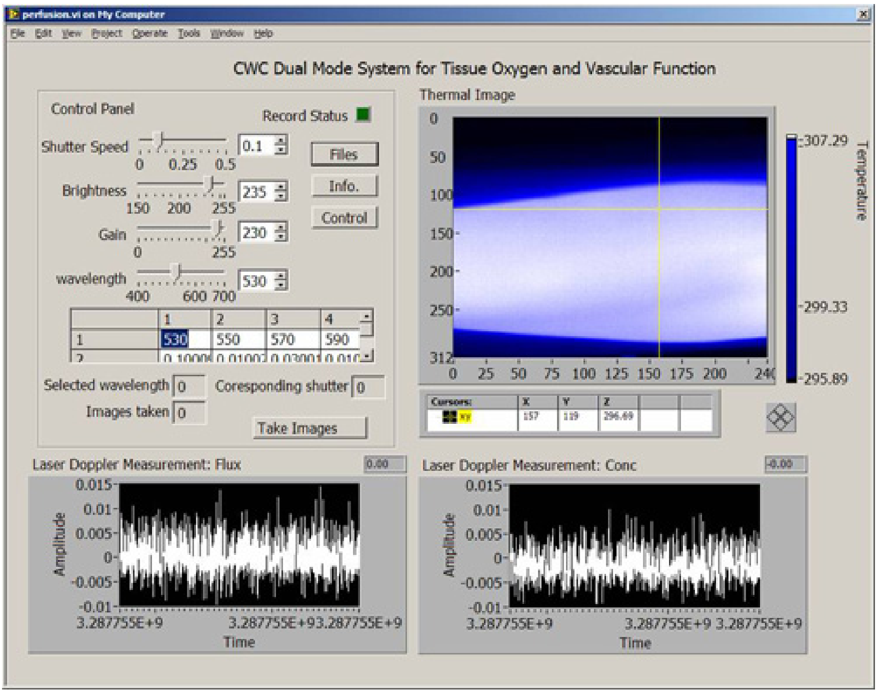

Figure 2. Software interface for the CWC system. The software interface was programmed in the Labview environment. On the top left of the interface is the control panel for hardware configuration and system calibration. On the right of the interface is the real-time display of the tissue temperature map acquired by the infrared camera. On the bottom of the interface are laser Doppler measurements of skin tissue perfusion.

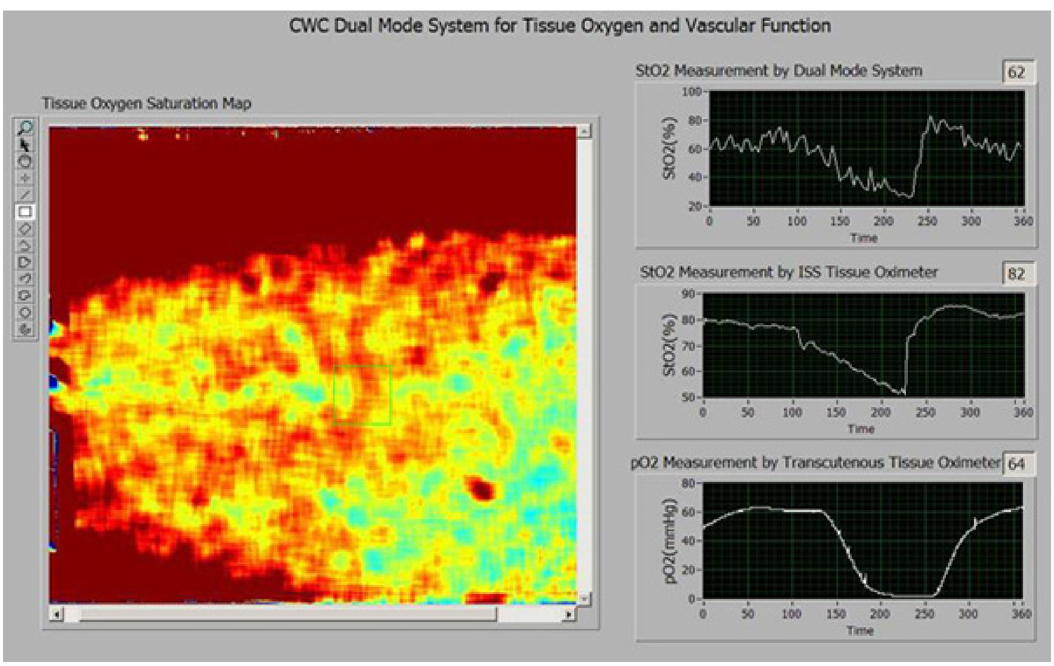

Figure 3. Software interface for the CWC system (Cont.). This is a pop-up window to show tissue oxygenation parameters. On the left is the tissue oxygenation map reconstructed from the multispectral images. The right side of the interface displays the following tissue oxygenation parameters from top down: (1) cutaneous tissue oxygenation averaged from a selected region of interest (ROI) in the tissue oxygenation map; (2) deep tissue oxygenation monitored by an OxplexTS tissue oximeter; (3) cutaneous tissue oxygen tension monitored by a TCM transcutaneous oxygen monitor.

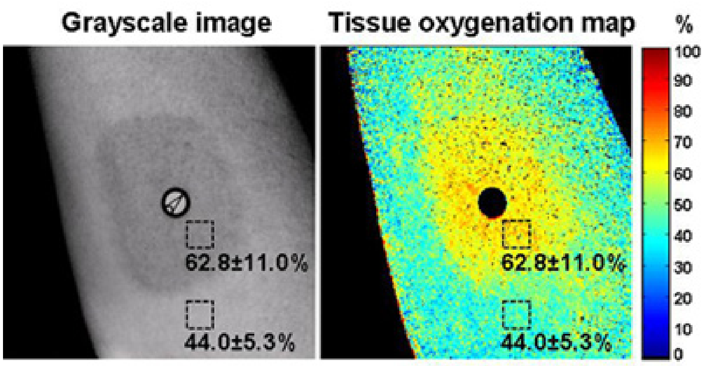

Figure 4. Cutaneous tissue oxygenation imaging by an OxyVu imaging system. The left figure is a grayscale image of the skin tissue. A layer of ink was painted on the skin to simulate the skin color. The map of cutaneous tissue oxygenation acquired by the OxyVu system is shown on the right. Two square-shaped regions of interest (ROIs) were selected within and outside the ink-painted area respectively. For the ROI within the ink-painted area, the averaged cutaneous tissue oxygenation was 62.8±11.0%. For the ROI outside the ink-painted area, the averaged cutaneous tissue oxygenation was 44.0±11.0%. A difference of 18.8% was observed for the cutaneous tissue oxygenation measurements within and outside the ink-painted skin area.

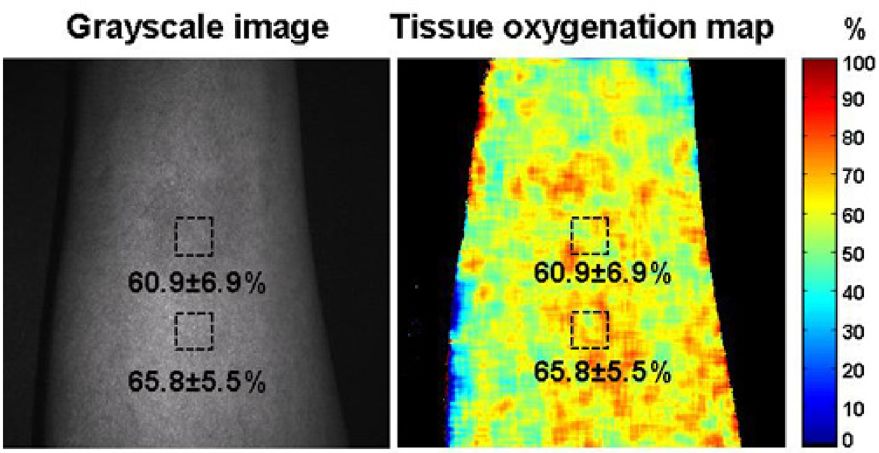

Figure 5. Cutaneous tissue oxygenation imaging by the CWC system. The multispectral images were captured by the CWC system at the same skin location on the same subject as that in Figure 4. The left figure is the single wavelength image of the skin tissue and the right figure is the reconstructed cutaneous tissue oxygenation map. A layer of ink was painted on the skin with the ink concentration the same as that in Figure 4. . Two square-shaped regions of interest (ROIs) were selected within and outside the ink-painted area respectively. For the ROI within the ink-painted area, the averaged cutaneous tissue oxygenation was 60.9±6.9%. For the ROI outside the ink-painted area, the averaged cutaneous tissue oxygenation was 65.8±5.5%. A difference of 4.9% was observed for the cutaneous tissue oxygenation measurements within and outside the ink-painted skin area.

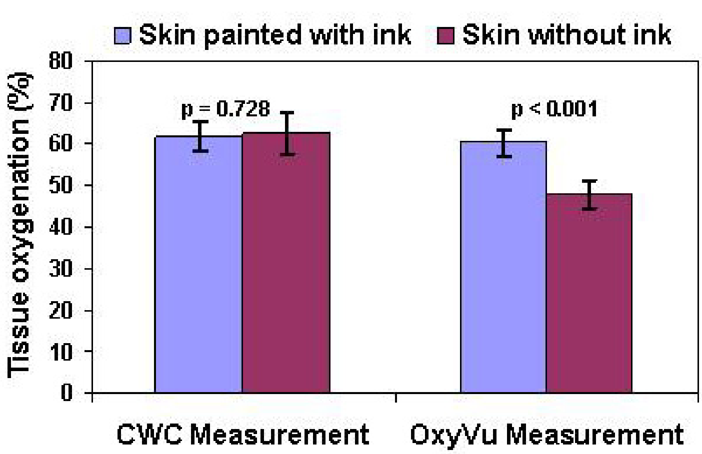

Figure 6. The effect of simulated skin color changes on the reliability of cutaneous tissue oxygenation measurements. Statistic analysis was carried out to determine the significance of the simulated skin color changes to oxygenation measurements for both the OxyVu and the CWC imaging systems. For each imaging system, the averaged cutaneous tissue oxygenations were calculated within and outside the ink-painted skin areas by randomly selecting 10 regions of interest (ROIs) in each area. Our null hypothesis is that the change of skin color will not

affect the cutaneous tissue oxygenation measurement. This null hypothesis was tested using oxygenation maps in Figure 4 (i.e., the OxyVu measurements) and Figure 5 (i.e., the CWC measurements) respectively. Student's t-tests show that the p value for the OxyVu measurements is much less than 0.001, implying that the null hypothesis is rejected. Therefore, the change of skin color does affect the cutaneous tissue oxygenation measurements in an OxyVu imaging system. In contrast, the p value for the CWC measurements is 0.728, implying the likelihood that the change of skin color does not affect the cutaneous tissue oxygenation measurements in a CWC imaging system.

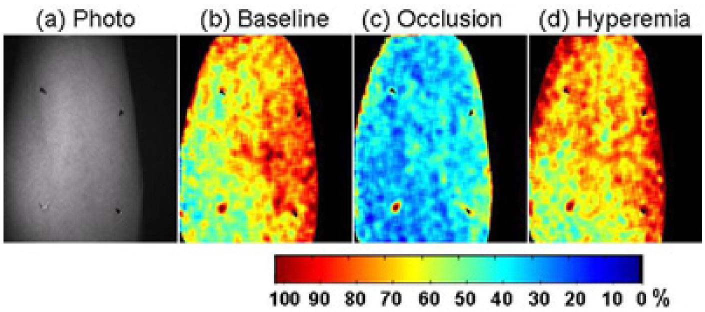

Figure 7. Cutaneous tissue oxygenation images obtained from the CWC system during post-occlusive reactive hyperemia (PORH). The PORH test was carried out on the forearm of a healthy subject following #1. (a). Single wavelength gray scale image of the arm with four fiduciary markers placed for image co-registration. (b) The baseline cutaneous tissue oxygenation map acquired before vascular occlusion. (c) The cutaneous tissue oxygenation map after vascular occlusion (systolic pressure + 50mmHg) for 2 minutes. (d) The cutaneous tissue oxygenation map after reactive hyperemia. Significant changes in cutaneous tissue oxygenation were observed before, during, and after vascular occlusion.

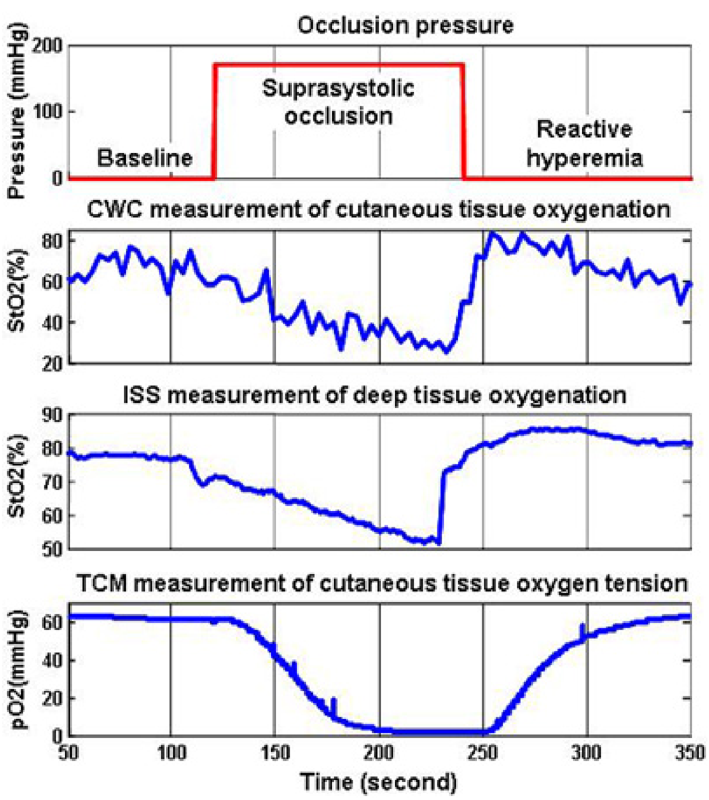

Figure 8. Tissue oxygen parameters continuously monitored during a PORH test. The test protocol in (a) shows a period of pre-occlusion baseline, followed by a suprasystolic occlusion period, and end with a reactive hyperemia period. The history of cutaneous tissue oxygenation duration the PORH procedure is plotted in (b). It was obtained by averaging a selected region of interest (ROI) in the CWC cutaneous oxygenation map. We also monitored the deep tissue oxygenation by an OxiplexTS tissue oximeter, as plotted in (c). The transcutaneous tissue oxygen tension was also monitored by a TCM device and plotted in (d). The CWC measurements of cutaneous tissue oxygenation coincide well with other oxygen parameters during the PORH procedure.

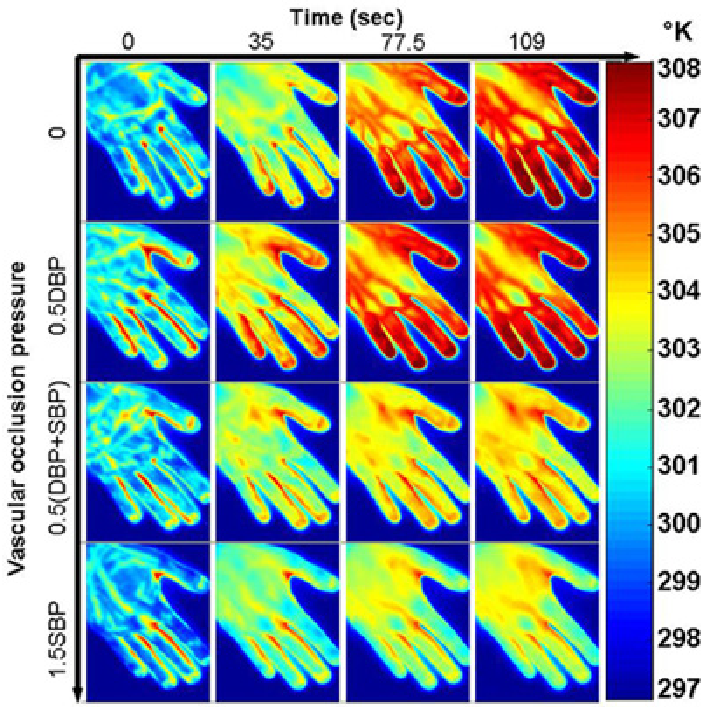

Figure 9. Cutaneous tissue responses at different vascular occlusion pressures. Thermographic images were acquired immediately after the thermal stimulation (i.e., a water bag at room temperature 25°C) was removed from the subject's left hand. The horizontal axis corresponds to the different time spots after the thermal stimulation was removed. The vertical axis corresponds to the following 4 levels of vascular occlusion pressures: 0 (No occlusion), 0.5DBP, 0.5(DBP+SBP), 1.5SBP, where DBP is the diastolic blood pressure and SBP is the systolic blood pressure. For this specific subject, the DBP is 69mmHg and the SBP is 123mmHg. The test results indicate that the tissue temperature response to the external thermal stimulation is correlated with the level of vascular occlusion. Increasing the occlusion pressure reduces the thermal response rate.

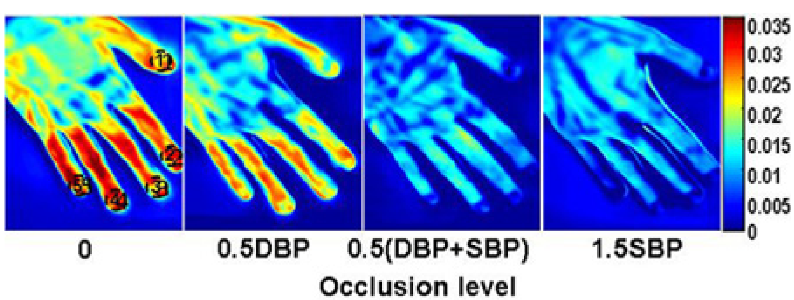

Figure 10. Reconstructed vascular index maps at different vascular occlusion pressures. Vascular function index (v) at each pixel of the thermographic images was derived by regressing the cutaneous tissue temperature change (ΔT) against the square root of the time after the thermal stimulation ($\sqrt{t}$): $\Delta \sqrt{t} + K + \varepsilon$, where ε is the random error and K is a constant. Vascular function index maps from left to right correspond to the following occlusion conditions: (a) no occlusion, (b) 0.5DBP, (c) 0.5 (DBP+SBP), (d) 1.5SBP. For this specific subject, the diastolic blood pressure (DBP) is 69mmHg and the systolic blood pressure (SBP) is 123mmHg.

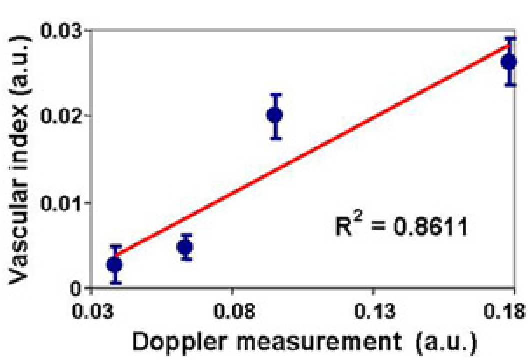

Figure 11. Correlation between the vascular function index and the skin tissue perfusion. The finger tip vascular function index at each occlusion pressure in #2 was calculated by averaging five regions of interest (ROIs) in the tissue vascular index map. The skin tissue perfusion

was measured by a laser Doppler device at one of the finger tip. The finger tip vascular index correlated with the laser Doppler measurement, indicating the potential of using the dynamic thermographic method for quantitative assessment of tissue vascular function.

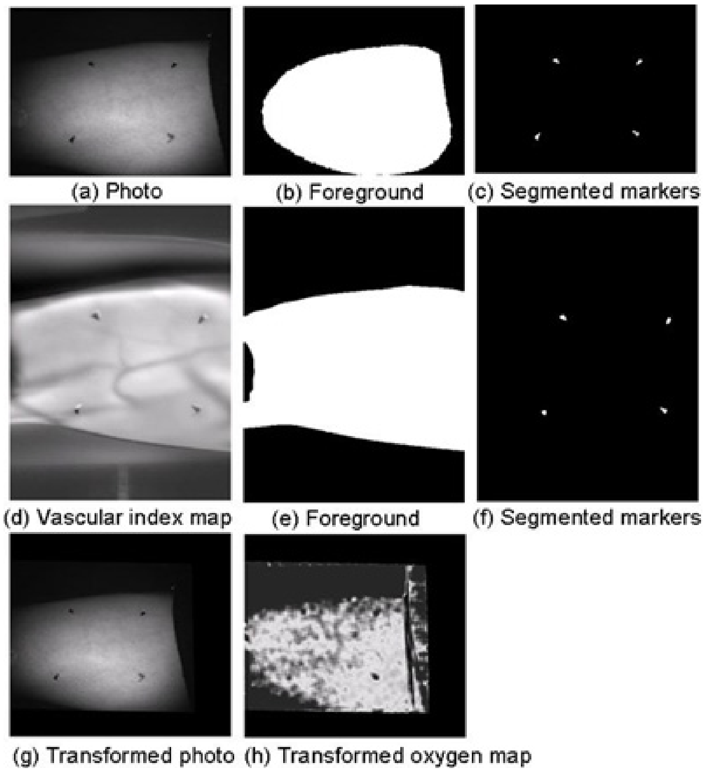

Figure 12. The image co-registration process. In the first row, we show: (a) the normalized photo, (b) the segmented foreground region, and (c) the segmented markers in the photo image. In the second row, we show: (d) the normalized perfusion map, (e) the segmented foreground region, and (f) the segmented markers in the perfusion map. The affine transformation between the two sets of marker positions was calculated. The co-registered images (g and h) were obtained by transforming the photo image and the oxygen map using this recovered affine transformation.

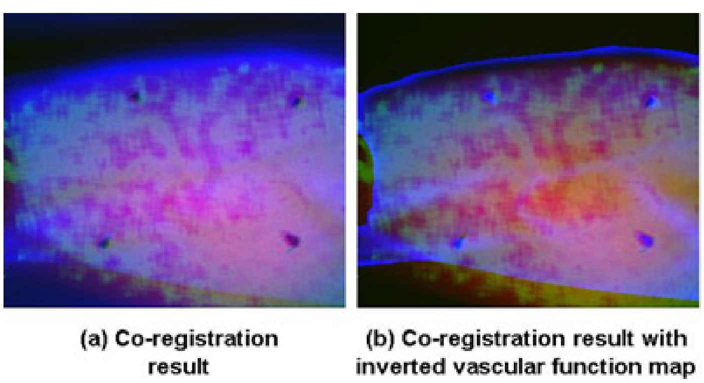

Figure 13. The co-registration results. The transformed photo and oxygen map, together with the perfusion map were co-registered and displayed in as a heat map. The heat map in (a) was presented with 100% of transformed photo image in the red channel, 100% of transformed oxygen image in the green channel and 50% of the perfusion map in the blue channel. In order to visualize the vessels better, we present another version of the co-registration result as in (b). The heat map was composed of 100% of transformed photo image in the red channel, 50% of transformed oxygen image in green channel, and 50% of changed perfusion map in the blue channel, where the vascular index map was inverted and only the information within the foreground region was kept.

Discussion

Oxygen exists in biological tissue in multiple forms such as hemoglobin or myoglobin bound oxygen, dissolved oxygen, and reactive oxygen species. Oxygen transport plays a critical role in maintaining tissue viability and normal metabolic processes [3]. Acute mild to moderate hypoxia will initiate metabolic adaptation, vascular regulation, and angiogenic responses [4]. Extreme hypoxia and anoxia will lead to insufficient angiogenesis and cell death. The imbalance between limited oxygen supply and increased oxygen demand is one of major causative factors for many disorders such as chronic wounds [5]. In the case of ischemic wounds, oxygen supply is limited by lack of perfusion and cannot meet the metabolic need of the healing process and compromising respiratory burst function aimed at fighting infection. Simultaneous assessment of cutaneous tissue oxygenation and vascular function has clinical significance in chronic wound management.

The hyperspectral imaging technique estimates cutaneous tissue oxygenation by illuminating tissue and detect tissue reflectance at different wavelengths [6]. One major advantage of hyperspectral imaging is non-invasive and non-contact detection of tissue functional properties. However, the oxygen measurement reliability for many hyperspectral imaging systems is affected by skin color and other background absorption variations. Wide gap second derivative spectroscopy was developed previously for tissue oxygenation measurement with minimal effect of scattering and skin pigmentation [1]. We applied the principle of the second derivative spectroscopy to multispectral imaging and demonstrated the consistent measurement of cutaneous tissue oxygenation independent with the simulated skin color changes.

Tissue perfusion was previously studied by measuring tissue thermal diffusivity [7]. A single hood method was developed to introduce thermal stimulation and image tissue dynamic responses in order to estimate the skin tissue thermal inertia distribution [8]. Experiments on human forearm skin subjected to arterial cuff occlusion demonstrated linear relationship between thermal inertia and blood perfusion measured by a laser Doppler imager before and during blood flow occlusion [8]. A lumped bioheat model was also used to estimate the finger tip vascular reactivity during venous occlusion plethysmography [9]. Despite the above efforts, quantifying skin blood perfusion from skin temperature measurements is challenging because of the lack of sensitivity, the dependence on subcutaneous fat thickness, and other contributing factors such as vasoconstriction, vasodilation, and motion artifacts [10]. In this protocol, we used an infrared camera to capture tissue temperature dynamics in response to a thermal stimulation at room temperature. The thermal stimulation was selected so that the effect of vasoconstriction and vasodilation was minimized. Further modeling and measurement efforts are necessary in order to delineate a reliable quantitative correlation between the vascular function index and the skin tissue perfusion.

In #3, we used the affine transformation for the co-registration tasks. However, given that the two cameras are positioned with different angles in the 3D space, it is potentially more accurate to apply a transformation related to the 3D transformation between the two cameras. Currently we are exploring in that direction which involve extrinsic calibration of the cameras in 3D space using epipolar geometry.

Disclosures

No conflicts of interest declared.

Acknowledgements

Supported by NIH awards RO1 HL073087, GM 077185, and GM 069589 to CKS. The work is also supported by a grant from the Regenerative Medicine program of the DHLRI. The authors are grateful to the technical support and clinical inputs from the following personnel at the Ohio State University: Dr. Sabyasachi.Biswas (Comprehensive Wound Center), Dr. Allison Spiwak (Circulation Technology Division), Joseph Agoston (Circulation Division), Thoma Shives (Circulation Division), Joseph Ewing (Mechanical Engineering), Scott Killinger (Mechanical Engineering), and Xiaoyin Ge (Electrical Engineering).

References

1. Myers, D.E., Anderson, L.D., Seifert, R.P., Ortner, J.P., Cooper, C.E., Beilman, G.J., et al. Noninvasive method for measuring local hemoglobin oxygen saturation in tissue using wide gap second derivative near-infrared spectroscopy. J Biomed Opt 10 (3) : 034017 (2005).
2. Jarm, T., Kragelj, R., Liebert, A., Lukasiewitz, P., Erjavec, T., Preseren-Strukelj, M., et al. Postocclusive reactive hyperemia in healthy volunteers and patients with peripheral vascular disease measured by three noninvasive methods. Adv Exp Med Biol 530 : 661-669 (2003).
3. Treacher, D.F., Leach, R.M. Oxygen transport-1. Basic principles. Bmj 317 (7168) : 1302-1306 (1998).
4. Leach, R.M., Treacher, D.F. Oxygen transport-2. Tissue hypoxia. BMJ 317 (7169) : 1370-1373 (1998).
5. Sen, C.K. Wound healing essentials: let there be oxygen. Wound Repair Regen 17 (1) : 1-18 (2009).
6. Greenman RL, Panasyuk S, Wang X, Lyons TE, Dinh T, Longoria L, et al. Early changes in the skin microcirculation and muscle metabolism of the diabetic foot. Lancet 366 (9498) : 1711-1717 (2005).
7. Valvano, J.W. The use of thermal diffusivity to quantify tissue perfusion. PhD thesis, Massachusetts Institute of Technology (1981).
8. Hassan, M., Togawa, T. Observation of skin thermal inertia distribution during reactive hyperaemia using a single-hood measurement system. Physiol Meas 22 (1) : 187-200 (2001).
9. Ley, O., Deshpande, C., Prapamcham, B., Naghavi, M. Lumped parameter thermal model for the study of vascular reactivity in the fingertip. J Biomech Eng 130 (3) : 031012 (2008).
10. Wilson, S.B., Spence, V.A. Dynamic thermographic imaging method for quantifying dermal perfusion: potential and limitations. Med Biol Eng Comput 27 (5) : 496-501 (1989).